www.gondwanags.org.in

Research Article

ISSN : 2455-1953

JGSR
Journal of Geosciences Research
Vol. 8, No.2, July, 2023, pp. 133-141

Geochemical Characteristics of Mafic Dykes from Wairagarh Area, Western Bastar Craton, Central India

S.B. Deshmukh[1], A.M. Pophare[1]*, Y.A. Murkute[1] and G.G. Wadpalliwar[2]

[1]*Department of Geology, RTM Nagpur University, Nagpur-440001(MS), India*
[2]*Shri Govindrao Munghate College of Art and Science, Kurkheda-441209(MS), India*
*(*Corresponding Author E-mail: apophare@gmail.com)*

Abstract

The NW-SE trending mafic dykes intrude the Amgaon gneisses and Dongargarh granite in Wairagarh area of the Western Bastar Craton (WBC). These dykes consist of mainly the clinopyroxene, plagioclase feldspar and minor amphiboles and titano-magnetite. These are metamorphosed to green schist facies. The mafic dykes show tholeiitic trend on multivariate geochemical plots and moderate range of variation in SiO_2 (50.15 to 52.84 wt.%), MgO (5.13 to 7.64 wt.%), Fe_2O_3 (12.97 to 15.08 wt.%), Al_2O_3 (12.74 to 14.48 wt.%) and the $Mg^{\#}$ value ranges from 37.74 to 51.21. Strong positive correlation of Sr, Th, Hf, U, Ga, Ta, Pb, Cs, Rb and HREEs negate the effect of post magmatic alteration. Negative Nb, Ta and Ti with positive Zr and Hf anomalies suggest the effect of assimilation and crustal contamination, which is also supported by Ce/Nb (0.23-0.33) equivalent to the crustal value. Negative ΔNb value suggests depleted mantle source for the mafic dykes of the WBC. Restricted range of $(Gd/Yb)_N$ (1.05-1.67), $(Dy/Yb)_N$ (0.94-1.25) and $(Sm/Yb)_N$ (1.22-2.26) advocate that these mafic dykes were derived from spinel lherzolite source. About 5-15% degrees of partial melting of depleted mantle source is envisaged for the generation of the mafic dykes. The field and geochemical evidences suggest that the mafic dykes of Wairagarh area, WBC were emplaced within continental rift environment.

Keywords: Mafic dykes, Geochemistry, Wairagarh, Bastar Craton, Central India.

Introduction

Geochemical investigation of mafic dyke swarms provide an adequate information about tectonic setting, their age of emplacement, depth of origin, *etc* (Rogers and Santosh, 2002; Srivastava and Gautam, 2012, 2015; Srivastava *et al.*, 2019). Emplacement of mafic dykes are related to mantle plume magmatism and associated continental rifting events (Halls, 1987; LeCheminant and Heaman, 1989; Ernst and Buchan, 1997; Bleeker and Ernst, 2006; Pearce, 2008; Ernst and Bleeker, 2010; Srivastava, 2011; Srivastava and Samal, 2019, Hazarika *et al.*, 2020). Mafic dykes intruded within the Archean cratons are studied by many workers (Murthy, 1987; Devaraju, 1995; Srivastava, 2008; Srivastava *et al.*, 2011).

Varieties of mafic dykes with their different geochemical characteristics were emplaced in varying geological time within the south, central as well as northern Bastar craton (Srivastava *et al.*, 1996; Srivastava and Singh, 2004; Srivastava, 2006; Subba Rao *et al.*, 2007, 2008; Gautam and Srivastava, 2011; Srivastava and Gautam, 2008, 2012, 2015; Chalapathi Rao and Srivastava, 2009; Ratre *et al.*, 2010; Das *et al.*, 2011; Chalapathi Rao *et al.*, 2011; Pisarevsky *et al.*, 2013; Srivastava *et al.*, 2016; Shellnutt *et al.*, 2018; Samal *et al.*, 2019; Liao *et al.*, 2019). However, the geochemical data on mafic dykes of the Central Bastar craton (Ramachandra *et al.*, 1995) and WBC (Alam *et al.*, 2009; Hazarika *et al.*, 2019, 2020) are scanty and are not studied in detail.

Present investigation is aimed to understand the geochemical nature, origin and evolution of NW-SE trending mafic dyke swarms exposed in and around the Wairagarh area of WBC that involves field relationship, petrography, geochemical features, tectonic setting and petrogenesis.

Geology

The Bastar craton covers an area of 1,30,000 km^2 and is bounded by the Godavari graben in the south, Mahanadi graben in the north-east, Central Indian Tectonic Zone (CITZ) forming part of the Satpuda mobile belt in the north, Eastern Ghats Mobile Belt (EGMB) in the east and Deccan Trap cover in the west. The triangular shaped Bastar craton covers parts of Chhattisgarh and Maharashtra States of Central India. The study area is located around Wairagarh area of Gadchiroli district, Maharashtra within Western Bastar Craton (Fig.1). The WBC includes all the litho tectonic components exposed west of Dongargarh granite batholiths (Table 1) comprising the Archean granulites, Neo-Archean to Palaeo-Proterozoic Bailadila and Bengpal groups, Amgaon gneisses and supracrustals, Dongargarh Supergroup,

(Received : 18 November 2022 ; Revised Form Accepted : 06 April 2023)
https://doi.org/10.56153/g19088-022-0132-31

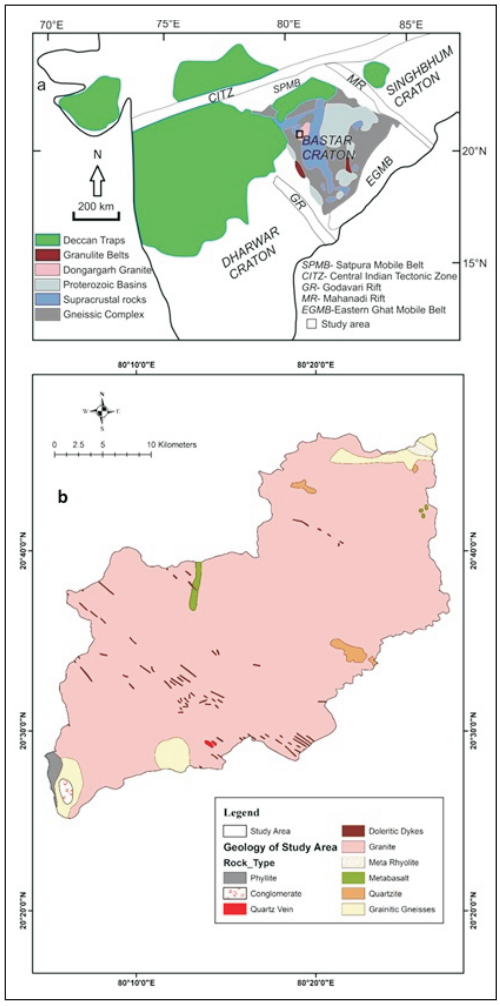

Fig. 1a. Generalized regional geological map of the Bastar Craton (*modified after* Yellappa et al. 2012); **b.** Geological map of study area (*modified after* DRM, GSI, 2001).

Sakoli Group, Wairagarh meta-sediments and younger sedimentary cover rocks of Meso-Proterozoic Pakhal Group (Sarkar *et al.*, 1990; Yellappa *et al.*, 2012).

The Amgaon Granitic Gneisses Complex (AGC) is the oldest lithological unit in the study area. These are pink to pinkish-white or greyish-white in colour, fine to coarse grained and are composed of resinous pink feldspar, quartz, amphibole and green mica. In the study area, the Amgaon gneisses are overlain by the quartzite of the AGC and underlain by the metabasalts of Bailadila Group. Metarhyolites of Nandgaon (Bijli) Group are unconformably overlain by the metabasalts of Bailadila Group and underlain by the Dongargarh Granite (GSI, 2001).

The Dongargarh Supergroup comprises the granite intrusives, dolerite dykes and quartz veins in major part of the study area. The granites intruded the Amgaon gneisses and Bijli rhyolites of the Nandgaon Group. The granites are composed of quartz, feldspar, hornblende and biotite. These are medium to coarse grained and grey to pink in colour. Mafic dyke swarms constitute a prominent cluster in the central part of the study area. Numerous intrusives such as dolerite and gabbro intrude within gneisses and granite. Generally, these bodies have a NW-SE to WNW-ESE trend. In the study area, the NW-SE to N-S trending mafic dyke swarms (Fig.1-2) of Wairagarh area extends from 200 m to 8 km in length,

Table 1: Stratigraphic succession of study area (GSI, 2001)

Groups (Age)	Litho-Units
Sakoli (1800-2000 Ma)	Phyllite Conglomerate
Dongargarh (2300 Ma)	Quartz Veins Doleritic Dykes Granite
Nandgaon (Bijli) (2400 Ma)	Meta Rhyolite
Bailadila (2500-2600 Ma)	Metabasalt
Amgaon (3000 Ma)	Quartzite Granitic Gneisses

with the width of 20-100 m. The mafic dykes cut across the Dongargarh granite with sharp contact. These dykes are doleritic, massive, hard and compact, grey to greenish black, fine to medium-grained and holocrystalline. Grain size varies from medium to coarse grained in the central part of the dyke rocks to relatively fine grained at the margins (Fig. 3a-b). The NW-SE trending quartz veins are well exposed in the south-eastern part of the study area near Uradi village, varying from 4 to 5 m in width and 10 m in length (GSI, 2001).

The Nandgaon Group is unconformably overlain by the Sakoli Group of rocks that consists of weakly metamorphosed sedimentary rocks comprising lenses of polymictic conglomerates, meta-arkose, thin quartzite and thin ferruginous quartzite bands. Together they have been termed as Wairagarh meta-sediments (Shashidharan *et al.*, 2002).

Petrography

The major minerals observed in the mafic dykes are clinopyroxene (augite) and plagioclase feldspar (albite). Subhedral to anhedral mineral grains of augite enclosing the laths of plagioclase partly or completely indicate sub-ophitic to ophitic texture (Fig. 3c-d). The glomeroporphyritic texture can also be identified (Fig. 3e). The average modal percentages of minerals are plagioclase feldspar: 30-50%, augite: 20-35%, hornblende: 3-5%, opaque (magnetite, ilmenite, chalcopyrite and pyrite): 2-4% and 1% of other minerals. Chlorite, actinolite and clinozoisite are found in the form of aphanitic matrix as secondary minerals (Fig.3d, e-f).

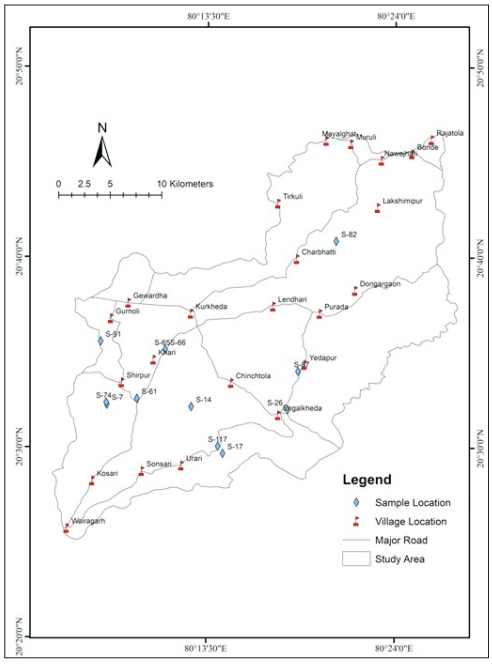

Fig.2. Sample location of study area.

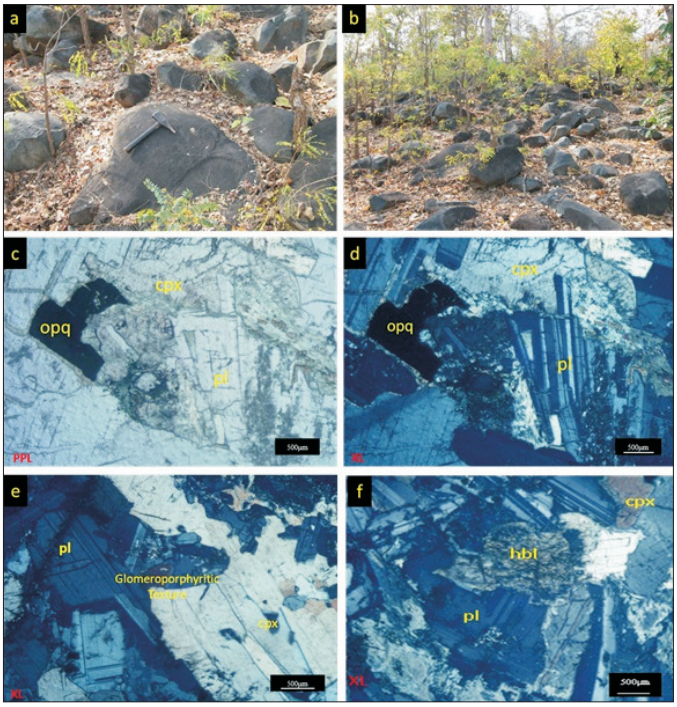

Fig. 3a-b. Field photographs of mafic dykes within study area; **c.** Photomicrographs showing development of opaque minerals (opq) (PPL); **d.** Opaque minerals (opq) (XL); **e.** Photomicrographs showing clinopyroxene (cpx), plagioclase (pl) and clusters of Pl that have developed a glomeroporphyritic texture (XL); **f.** Small Pl laths penetrating cpx, reflecting their ophitic relationship and hornblende (hbl) (XL)**.**

Sericitization, uralitization and saussuritization are also evident within these dykes. Secondary minerals such as sericitized feldspar, uralitized pyroxene, amphiboles and chlorite *etc* are observed. These secondary minerals represent low to medium grade metamorphism of the mafic dykes.

Results and Discussion

A total seventy-seven dyke rock samples were collected from the study area. Sampling was done in the middle portion of the dyke to avoid altered samples. Out of which twelve fresh (unaltered) samples are selected for whole rock geochemical investigation (Fig. 2). Samples were powdered to -250 mesh size. The geochemical analyses were carried at CSIR-National Geophysical Research Institute (NGRI) Hyderabad. Major elements were analysed by Philips MAGIX PRO Model 2440 X-ray fluorescence spectrometry (XRF). Trace elements and REE were analysed using a Perkin Elmer SCIEX ELAN DRC II High Resolution-Inductive Coupled Plasma Mass-Spectrometry (HR-ICP-MS). International standard BHVO-1 was used as reference materials (Balaram and Naneshwar Rao, 2003).

The SiO_2 shows variation from 50.15 to 52.84wt.% and TiO_2 varies from 0.47 to 0.96wt.%. Al_2O_3 varies from 12.74 to 14.48wt.%. Fe_2O_3 from 12.97 to 15.08wt.%, MnO from 0.17 to 0.19wt.%, whereas MgO shows a wide variation from 5.13 to 7.64wt.%. CaO varies from 9.08 to 10.85wt.%, Na_2O from 1.83 to 2.34wt.%, K_2O from 0.49 to 1.17wt.% and P_2O_5 show variation between 0.13 and 0.28wt.%. $Mg^{\#}$ varies from 37.74 to 51.21. $Mg^{\#}$ is moderate to low indicating evolved nature of dykes (Table 2).

The studied mafic dyke can be classified as sub-alkaline

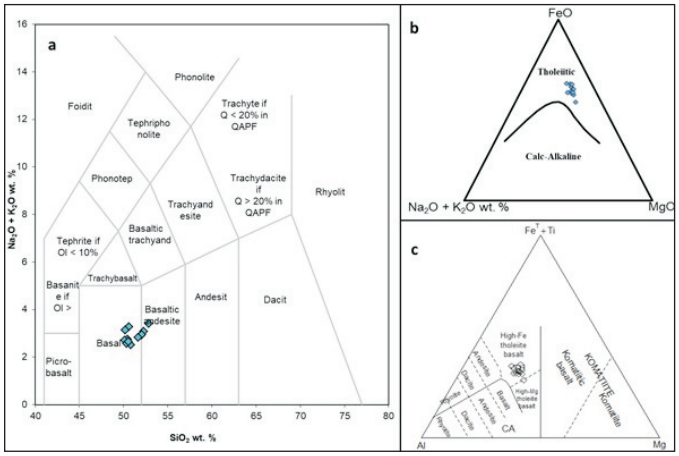

Fig. 4a. Total-alkali silica (TAS) diagram (*after* Le Bas et al., 1986); **b.** AFM triangular plot (*after* Irvine and Baragar, 1971); **c.** Triangular cationic plot (*after* Jensen, 1976).

basalt and basaltic andesite in terms of total alkali silica (TAS) components (Fig.4a; Le Bas *et al.*, 1986). In the AFM diagram (Irvine and Baragar, 1971), all dykes clustered in the tholeiitc field (Fig.4b). The dykes fall in the field of high-iron tholeiite (HFT) on cation parameters of Jensen (1976; Fig.4c).

$Mg^{\#}$ shows negative correlation with Fe_2O_3, TiO_2 and P_2O_5 (Fig.5a). All the other oxides show no correlation with $Mg^{\#}$. The trace elements such as Co and Ni show negative correlation with $Mg^{\#}$ but other trace elements show scatter (Fig.5b). All the REEs show negative correlation with $Mg^{\#}$, except for the Nd, Tm, Yb and Lu (Fig.5b). Based on the observed positive correlation of major oxides, trace elements and REEs it is suggested that most of the elements are found to be immobile during post magmatic alteration, and hence these immobile elements are used for further petrogenetic inference.

Mafic dykes in comparison with volcanic rocks are found to be least contaminated, however contamination of extruding magma with crustal material cannot be negated (Mohr, 1987; Tarney and Weaver, 1987). The multielement spidergram of mafic dykes reflects negative Nb, Ta, Th and Ti anomalies (Fig.6a), whereas Zr and Hf show positive anomalies that indicating crustal contamination (Zhao and Zhou, 2007; Cai *et al.*, 2010). The LREEs are fractionated and show enriched pattern as compared to the MREEs and HREEs, which show flat pattern (Fig.6b). Negative Nb and Ta anomalies with enriched LREEs indicate crustal contamination, whereas in some mantle derived high-Mg derivatives negative Nb and Ta anomalies are observed that counter the crustal contamination (Cameron *et al.*, 1983; Hall and Hughes, 1987; Poidevin, 1994; Smithies, 2002; Srivastava, 2006, 2008). However, Nb/La (0.52-0.74) and Nb/Ce (0.23-0.33) of the mafic dykes are found to be close to the average crustal values (Nb/La = 0.46 and Nb/Ce = 0.23) (Weaver and Tarney, 1984), which relates these mafic dykes to have undergone the crustal contamination (Table 3).

The mafic dykes of WBC were originated from the spinel lherzolite field of depleted mantle source (Lassiter and DePaolo, 1997; Fig.7a,b). The negative trend in $(La/Sm)_N$ vs. $(Nb/La)_N$ (Fig.7c), $(La/Sm)_N$ vs. $(Nb/Th)_N$ (Fig.7d) and Zr/Y vs. $(Nb/Th)_N$ (Fig.7f) plots, clearly reflects the crustal mixing of magma that was derived from a relatively depleted mantle source. In a Nd vs. Ce variation plot (Fig.7e), the trend line of studied dyke sample

Table 2: Whole-rock major oxide (wt.%), trace and rare-earth element composition of mafic dykes of WBC.

Sample	S-7	S-14	S-17	S-26	S-61	S-65	S-66	S-74	S-82	S-87	S-91	S-117
Latitude	20° 32' 14.64"	20° 32' 8.52"	20° 29' 40.92"	20° 31' 59.88"	20° 32' 33.72"	20° 35' 8.52"	20° 35' 8.52"	20°32'21.48"	20° 40' 51.6"	20° 34' 0.48"	20° 35' 34.08"	20° 30' 3.6"
Longitude	80° 7' 55.44"	80° 12' 37.56"	80° 14' 23.46"	80° 18' 0.97"	80° 9' 35.46"	80° 11' 10.02"	80° 11' 10.02"	80° 7' 53.4"	80° 20' 42"	80° 18' 35.1"	80° 7' 33.66"	80° 14' 7.27"
Major oxides (Wt.%)												
SiO_2	50.60	50.44	50.15	52.28	50.83	52.84	52.03	52.06	50.35	50.54	50.19	51.63
TiO_2	0.47	0.67	0.76	0.86	1.34	0.70	0.74	0.76	0.72	0.92	0.96	0.70
Al_2O_3	14.39	14.48	14.29	13.16	12.74	14.19	13.65	13.43	14.25	14.10	14.25	13.95
Fe_2O_3	12.97	14.65	14.96	13.59	15.04	13.43	14.08	13.59	13.75	14.41	15.08	13.62
MnO	0.18	0.18	0.17	0.19	0.19	0.18	0.18	0.19	0.18	0.18	0.18	0.18
MgO	7.64	5.95	5.55	6.23	5.92	5.64	6.14	6.74	6.06	6.38	5.13	6.36
CaO	9.67	10.18	10.37	9.08	9.94	9.09	9.43	9.69	10.85	9.94	9.52	9.56
Na_2O	2.10	2.09	2.16	2.14	1.83	2.34	2.14	2.20	2.08	2.01	2.15	2.00
K_2O	1.17	0.65	0.55	0.93	0.69	1.07	0.78	0.74	0.49	0.63	0.98	0.82
P_2O_5	0.13	0.17	0.17	0.20	0.21	0.23	0.23	0.19	0.17	0.15	0.28	0.16
Mg#	51.21	41.98	39.79	44.96	41.22	42.80	43.73	46.92	43.99	44.10	37.74	45.42
Trace elemants (ppm)												
Cr	182.76	198.01	178.97	233.19	260.38	163.60	204.86	199.57	183.91	237.44	193.97	182.79
Ni	125.09	140.62	159.61	141.07	154.21	123.54	139.73	110.13	104.70	137.20	114.65	123.50
Co	49.65	51.57	59.92	54.54	57.04	48.54	50.75	48.10	43.56	50.51	53.87	46.83
Sc	37.56	38.46	44.77	42.22	42.23	38.39	38.41	37.70	35.31	37.18	37.38	35.14
V	354.18	307.20	429.76	302.43	311.56	323.71	339.27	337.17	296.78	464.94	284.64	306.40
Cu	191.78	172.68	222.91	200.57	132.25	143.79	148.64	280.57	148.68	237.80	105.15	173.55
Pb	3.05	3.10	5.79	3.46	2.56	2.57	3.08	3.48	1.94	2.82	2.09	4.05
Zn	51.14	73.81	135.88	131.24	153.84	96.36	95.03	81.70	53.19	57.77	76.07	86.19
Rb	50.21	35.32	35.03	37.71	23.38	35.31	27.70	28.01	23.26	24.99	31.00	30.08
Cs	0.26	0.37	0.44	0.30	0.20	0.26	0.22	0.22	0.24	0.22	0.21	0.26
Ba	162.29	183.99	210.79	267.54	153.93	228.09	215.05	201.69	119.53	156.47	237.03	247.66
Sr	199.27	208.64	238.73	237.64	167.33	196.22	177.43	184.20	164.58	165.27	219.51	188.45
Th	1.59	2.08	2.51	2.68	1.71	1.81	1.56	1.49	1.22	1.29	2.03	1.93
U	0.89	1.06	1.28	0.77	0.54	0.69	0.60	0.67	0.61	0.60	0.62	0.77
Ga	26.54	29.29	35.32	24.86	19.13	21.87	21.71	22.08	21.17	20.82	20.61	24.04
Ta	0.83	1.11	1.32	0.97	0.80	0.86	0.83	0.75	0.71	0.64	0.82	0.87
Nb	5.70	8.07	9.41	9.45	9.22	7.10	6.73	5.98	5.36	5.83	9.77	7.60
Hf	9.86	11.67	13.99	8.37	5.38	7.03	6.05	7.30	6.67	6.37	6.11	8.35
Zr	376.22	437.50	521.77	342.78	199.88	266.66	253.13	272.87	249.69	242.10	227.17	325.95
Ti	0.28	0.40	0.46	0.52	0.80	0.42	0.44	0.46	0.43	0.55	0.58	0.42
Y	24.99	35.00	40.35	32.92	34.21	32.29	32.86	29.72	26.94	23.67	32.18	30.85
P	0.06	0.07	0.07	0.09	0.09	0.10	0.10	0.08	0.07	0.07	0.12	0.07
Rare earth elements (ppm)												
La	10.19	14.17	16.66	17.13	12.49	13.31	13.02	11.00	8.99	9.13	15.63	13.37
Ce	22.95	31.08	36.62	36.50	28.13	28.78	28.71	24.87	20.15	20.52	34.67	30.24
Pr	2.97	4.09	4.77	4.63	3.85	3.77	3.83	3.34	2.75	2.64	4.50	3.94
Nd	12.77	15.33	18.29	18.92	14.91	14.64	16.83	14.77	11.29	10.24	17.00	16.83
Sm	2.99	4.14	4.70	4.33	4.28	3.82	4.05	3.69	3.06	2.74	4.57	4.01
Eu	0.87	1.22	1.40	1.28	1.36	1.12	1.20	1.12	1.00	0.90	1.45	1.12
Gd	3.40	4.83	5.52	4.78	5.27	4.62	4.64	4.29	3.79	3.31	5.31	4.51
Tb	0.59	0.85	0.98	0.82	0.91	0.80	0.81	0.74	0.67	0.59	0.88	0.78
Dy	3.75	5.30	6.12	5.04	5.60	5.05	5.08	4.74	4.21	3.77	5.26	4.79
Ho	0.85	1.19	1.37	1.11	1.20	1.11	1.12	1.02	0.93	0.82	1.13	1.06
Er	2.40	3.37	3.89	2.97	3.21	3.05	2.99	2.86	2.56	2.31	2.96	2.83
Tm	0.40	0.53	0.63	0.47	0.48	0.46	0.45	0.44	0.39	0.36	0.44	0.44
Yb	2.68	3.68	4.28	3.18	3.12	3.11	2.96	2.94	2.65	2.42	2.89	3.04
Lu	0.39	0.54	0.62	0.46	0.45	0.45	0.43	0.43	0.39	0.35	0.42	0.44

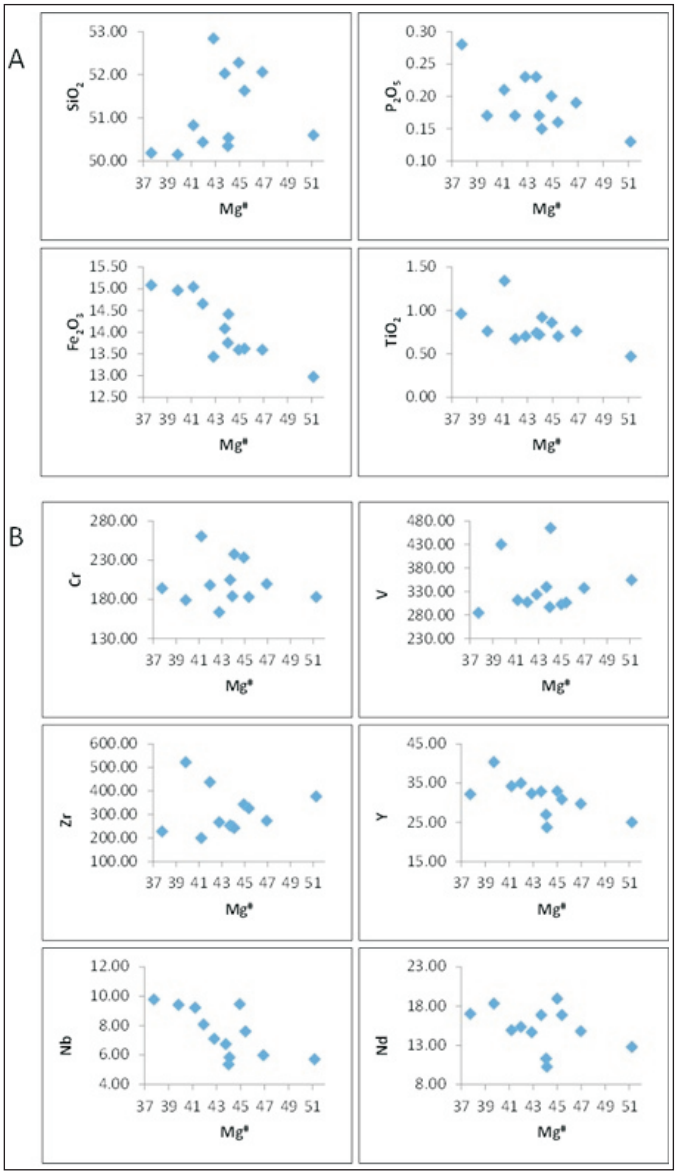

Fig.5a. Harker variation diagram for $Mg^{\#}$ *vs* wt.% Oxides; **b.** Harker variation diagram for $Mg^{\#}$ *vs*. Trace elements.

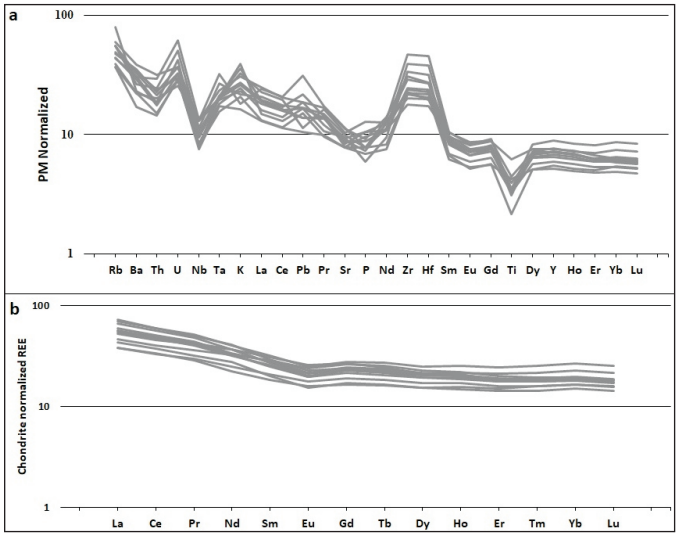

Fig. 6a. Primordial mantle-normalized multi-element spider-diagrams (normalising values taken from McDonough *et al.*, 1992 and Evensen *et al.*, 1978); **b.** Chondrite-normalized rare-earth element patterns for the mafic dykes from the WBC.

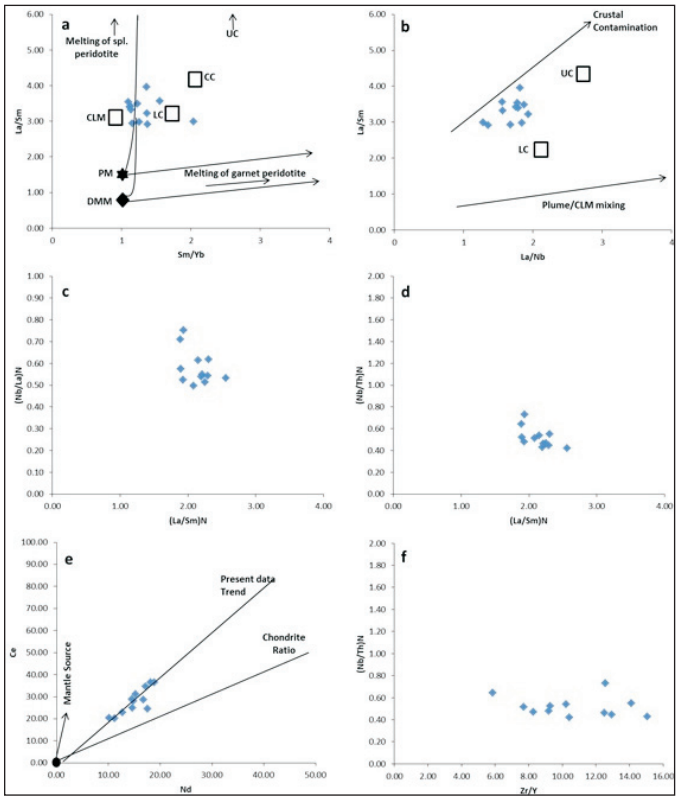

Fig. 7a Sm/Yb *vs*. La/Sm plot of mafic dykes in WBC; PM: Primitive Mantle; DMM: Depleted MORB mantle; CLM: Continental lithospheric mantle; UC: Upper crust; CC: Bulk continental crust; LC: Lower crust. (*fields after* Lassiter and DePaolo, 1997); **b.** La/Nb *vs*. La/Sm plot of mafic dykes in WBC; fields are those of Lassiter and DePaolo (1997); **c.** $(La/Sm)_N$ *vs*. $(Nb/La)_N$ plot of mafic dykes in WBC; **d.** $(La/Sm)_N$ *vs*. $(Nb/Th)_N$ plot of mafic dykes in WBC; **e.** Nd *vs*. Ce plot of mafic dykes in WBC (*after* Horan *et al.*, 1987); **f.** Zr/Y *vs*. $(Nb/Th)_N$ plot of mafic dykes in WBC.

intersect the Nd axis above the chondrite value, which indicate that the crustal contamination and assimilation-cum-fractional crystallization (AFC) were dominant processes during the origin and extrusion of these mafic dykes (Ahmed and Tarney, 1991). Moreover, the relatively low values of Nb/Th, Nb/La and high Zr/Y, La/Sm ratios of the mafic dykes indicate dominant role of crustal contamination during their extrusion. These ratios further indicate low pressure melting of the continental crust by the incoming heat of underplated basaltic magma (Arndt and Jenner, 1986; Puchtel *et al.*, 1997, 1998).

It is difficult to distinguish the possible occurrences of rift or arc tectonic environment (Crawford, 1989; Hatton and Sharpe, 1989; Piercey *et al.*, 2001; Asthana *et al.*, 2018). A wide range of chemical composition is observed for island arc basalt (IAB) due to the mixture of three components *viz.*, basaltic oceanic crust, a wedge of upper mantle and subducted sediments (Neogi *et al.*, 1996; Ellam and Hawkesworth, 1988; McDermott *et al.*, 1993). Moreover, the mafic dykes of Southern Bastar craton (SBC) (Shrivastava and Singh, 2004) and rocks from the Gulf of California were perfectly rift related rocks but show IAB and continental arc signatures (Paz Moreno and Demant, 1999). Various incompatible trace elements of mafic dykes are used to interpret tectonic setting

Table 3: Elemental ratios of litologies of Bastar craton, primordial mantle and crust

Source	Nb/La	Nb/Ce	(La/Sm)N	Reference
Mafic Dykes, WBC	0.52-0.74	0.23-0.33	1.82-2.47	Present Work
Granitoids, SBC	0.36	0.23	5.75	Hsean *et al.* (2003)
Primordial Mantle	1.01	0.39	1	McDonough et al. (1992)
Crust	0.46	0.23	4.25	Weaver and Tarney (1984)

of WBC. The Zr *vs* Ti plot (Fig.8a) show that all the dykes plot within plate or close to the within plate field, whereas the Zr *vs* Zr/Y plot (Fig.8b) shows that all dykes plot within the continental plate field (Pearce and Norry, 1979). This indicates that the mafic dykes of WBC were emplaced within the continental rift tectonic environment.

The LILEs and LREEs are found to be enriched in magma due to their interaction with enriched components of crust (Arndt and Jenner, 1986; Fitton *et al.*, 1997; Hawkesworth and Gallager, 1993; Puchtel *et al.*, 1997, 1998). Whereas, the highly incompatible elements are least affected by the contamination and more likely indicate a feature of source (Albarede, 1996). Therefore, highly incompatible HFSE (Nb) and trace element (U) are used to study the source-melt characteristics. The Nb/U ratio of the mafic dyke ranges from 6.41 to 17.22 and Zr *vs* Nb plot (Fig.9a) represents the depleted mantle source for the origin of the mafic dykes of WBC.

According to Fitton *et al.* (1997) ΔNb is considered to be most robust and diagnostic tool than the isotopic ratios for identifying the mantle source of varying degrees of altered and contaminated basalts. It is immobile during variable degrees of partial melting, crustal contamination and post magmatic alteration (Fitton *et al.*, 1997; Kent and Fitton, 2000). The calculated ΔNb of mafic dykes of WBC ranges from - 0.30 to - 1.16, which indicate depleted mantle source for the origin of mafic dykes of the study area.

The observed restricted range of ratios Gd/Yb_N (1.05-1.67), Dy/Yb_N (0.94-1.25) and Sm/Yb_N (1.22-2.26) are indicative of absence of garnet in the mantle source. The Sm/Yb vs. La/Sm plot (Fig.7a) shows the composition of mantle source as spinel lherzolite (Haase, 1996; Lassiter and DePaolo, 1997).

The magma with low value of $(Dy/Yb)_N$ (1.05-1.67) and high SiO_2 (48.78-52.84) is generated at low pressure of melting (Green, 1971; Frey *et al.*, 1978; Haase, 1996; Geldmacher *et al.*, 1998; Fig.9b). The average pressure estimates (*after* Haase, 1996) at which the mafic dykes instigate was ~10.36 Kbar, which indicate that the mafic dykes in the WBC were originated at low pressures (shallower depth equivalent ~ 35 to ~ 45 km) of mantle melting in the spinel lherzolite field (Haggerty, 1995).

The degree and depth of melting and AFC creates huge impact on the content of major elements, especially on trace elements of dyke magma. Incongruous behaviour of Ni (compatible) and Ce (incompatible) is used to identify the melting and crystallization processes (Allègre and Minster, 1978) on Ni *vs* Ce plot (Fig.10; Vijaya Kumar *et al.*, 2018). The mantle source assumed for the batch melting calculations has 1900 ppm Ni and 1.6 ppm Ce with the bulk distribution coefficient (D) for Ni is 4 and 0.0015 for Ce. Similarly, the 'D' values for the FC and AFC calculations are 6 and 0.02 for Ni and Ce, respectively. It is observed that the primary melts for mafic dykes of WBC should have been formed by around ~5 to ~15% degrees of partial melting of a mantle

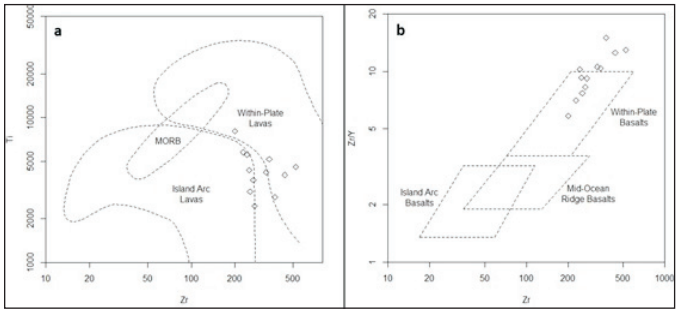

Fig.8. Tectonic Discriminate plots: **a.** Zr *vs* Ti plot (*after* Pearce, 1982); **b.** Zr *vs*. Zr/Y plot (*after* Pearce and Norry, 1979).

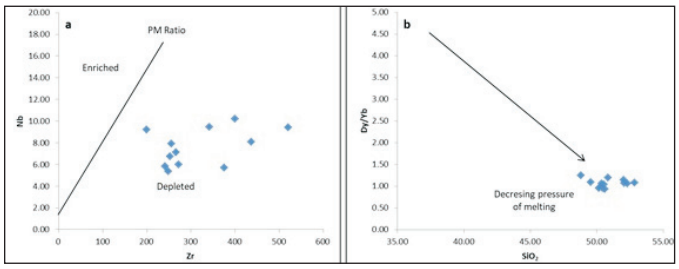

Fig. 9a. Zr *vs*. Nb plot of mafic dykes in WBC (*after* Ahmed and Tarney, 1991); **b.** SiO_2 *vs*. $(Dy/Yb)_N$ plot of mafic dykes in WBC.

sources (Fig.10). These estimated degree of partial melting can be correlated very well with average estimate melting range of rift related basaltic magma (5-10%; Herzberg, 1992, 1995; Geldmacher *et al.*, 1998).

Conclusions

Mafic dykes from Western Bastar Craton are classified as basalt and basaltic andesite of sub-alkaline series. It can be characterized as low MgO and Cr with flat HREE pattern. Trace including the REE distribution patterns of mafic dykes suggest fractionation of magma derived from depleted mantle source (-ΔNb values). Low range of $Mg^{\#}$ with negative Nb, Ta and Ti anomalies and positive Zr, Hf anomaly indicates crustal contamination. The mafic dykes of WBC show within continental plate rift tectonic setting during its origin and extrusion. The mafic dykes of WBC can be generated by ~5 to ~15% partial melting of a spinel lherzolite mantle sources at ~10.36 Kbar pressure analogous to shallower depth equivalent of ~ 35 to ~ 45 km.

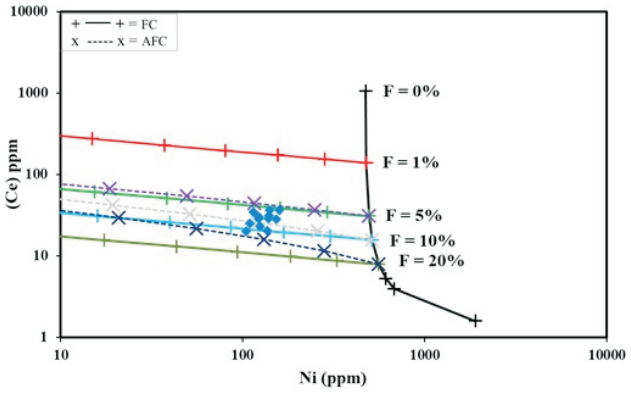

Fig.10. Ni *vs* Ce plot of mafic dykes in WBC (*after* Vijaya Kumar *et al.*, 2018).

Authors' Contributions

SBD: Field work, Data Collection and Data Generation, Investigation, Writing-Original Draft. **AMP**: Conceptualization, Visualization, Supervision and Formal Analysis, Reviewing and Editing. **YAM**: Methodology, Supervision and Formal Analysis. **GGW**: Data Collection and Data Generation, Investigation.

Conflict of Interest

Authors declare no conflicts of Interest.

Acknowledgements

This work was initiated under the supervision of (Late) Dr. H. S. Kale, Department of Geology, RTM Nagpur University, Nagpur. His untimely sad demise on 14th April 2022 has whacked the process for some time. SBD and GGW are highly indebted to, while AMP and YAM pay homage to (Late) Dr. H. S. Kale. SBD is thankful to the Director, NGRI and the In-charge Geochemistry Division for their help in obtaining the geochemical data.

References

Ahmad, T. and Tarney, J. (1991). Geochemistry and petrogenesis of Garhwal volcanics: implication for evolution of north Indian lithosphere. Precamb. Res., v. 50, pp. 69-88.

Alam, M., Naushad, M., Wanjari, N. and Ahmad, T. (2009). Geochemical characterization of mafic magmatic rocks of the central Indian shield: implication for Precambrian crustal evolution. Jour. Virt. Expl., v. 32(8), pp.1-20.doi:10.3809/jvirtex.2009.00246

Albarede, F. (1996). Introduction to the geochemical modeling. Cambridge University Press, v. 60, 537p.

Allegre, C.J. and Minster J.F. (1978). Quantitative models of trace element behavior in magmatic processes. Earth Planet. Sci. Lett., v. 38, pp. 1-25.

Arndt, N.T. and Jenner, G.A. (1986). Crustly contaminated komatites and basalt from Kambalda, Western Australia. Chem. Geol., v. 56, pp. 229-255.

Asthana, D., Kumar, S., Vind, A.K., Zehra, F., Kumar, H. and Pophare, A.M. (2018). Geochemical fingerprinting of ~2.5 Ga forearc-arc-backarc related magmatic suites in the Bastar Craton, Central India. Jour. Asian Earth Sci., v. 157, pp. 218-234. doi:10.1016/j.jseaes.2017.10.006

Balaram, V. and Naneshwar Rao, T. (2003). Rapid determination of REEs and other trace elements in geological samples by microwave acid digestion and ICP-MS. Atom. Spectro., v. 24, pp. 206-212.

Bleeker, W. and Ernst, R.E. (2006). Short-lived mantle generated magmatic events and their dyke swarms: the key unlocking Earth's paleogeographic record back to 2.6 Ga. *In*: Hanski, E., Mertanen, S., Rämö, T. and Vuollo, J. (*Eds.*), Dyke swarms- time markers of crustal evolution. Taylor & Francis, London, pp. 3-26.

Cai, K., Sun, M., Yuan, C., Zhao, G., Xiao, W., Long, X. and Wu, F. (2010). Geochronological and geochemical study of mafic dykes from the northwest Chinese Altai: implications for petrogenesis and tectonic evolution. Gond. Res., v. 18, pp. 638-652.

Cameron, W.E., McCulloch, M.T. and Walker, D.A. (1983). Bonninite petrogenesis: chemical and Nd-Sr isotopic constraints. Earth Planet. Sci. Lett., v. 65, pp. 75-89.

Chalapathi Rao, N.V. and Srivastava, R.K. (2009). A new find of boninite dyke from the Paleoproterozoic Dongargarh Supergroup: inference for a fossil subduction zone in the Archaean of the Bastar craton, Central India. Neues Jahrb. Mineral Abh., v. 186(3), pp. 271-282.

Chalapathi Rao, N.V., Burgess, R., Lehmann, B., Mainkar, D., Pande, S.K., Hari, K.R. and Bodhankar, N. (2011). $^{40}Ar/^{39}Ar$ ages of mafic dykes from the Mesoproterozoic Chhattisgarh basin, Bastar craton, Central India: implication for the origin and spatial extent of the Deccan large igneous province. Lithos, v. 125, pp. 995-1005.

Crawford, A.J. (1989). Boninites and Related Rocks. Unwin Hyman, London, v. 9, 465p.

Das, P., Das, K., Chakraborty, P.P. and Balakrishnan, S. (2011). 1420 Ma diabasic intrusives from the Mesoproterozoic Singhora group, Chhattisgarh Supergroup, India: implications towards non-plume intrusive activity. Jour. Earth Syst. Sci., v. 120, pp. 223-236.

Devaraju, T.C. (1995). Dyke swarms of peninsular India. Geol. Soc. India, Memoir No. 33,

Ellam, R.M. and Hawkesworth, C.J. (1988). Elemental and isotopic variations in subduction related basalts: evidence for a three component model. Contrib. Miner. Petrol., v. 98, pp. 72-80.

Ernst, R.E. and Bleeker, W. (2010). Large igneous provinces (LIPs), giant dyke swarms, and mantle plumes: significance for breakup events within Canada and adjacent regions from 2.5 Ga to the present. Can. Jour. Earth Sci., v. 47, pp. 695-739.

Ernst, R.E. and Buchan, K.L. (1997). Giant radiating dyke swarms: their use in identifying pre-Mesozoic large igneous provinces and mantle plumes. In: Mahoney, J. and Coffin, M. (Eds.), Large igneous provinces: continental, oceanic, and planetary volcanism. Geophys. Monogr. Ser., v. 100, pp. 297-333.

Evensen, N.M., Hamilton, P.J. and O'Nion, R.K. (1978). Rare earth abundances in chondritic meteorites. Geochim. et. Cosmochim. Acta, v. 42, pp. 1199-1212.

Fitton, J.G., Saunders, A.D., Norry, M.J., Hardarson, B.S. and Taylor, R.N. (1997). Thermal and chemical structure of the Iceland plume. Earth Planet. Sci. Lett., v. 153, pp. 197-208.

Frey, F.A., Green, D.H. and Roy, S.D. (1978). Integrated models of basalt petrogenesis: a study of quartz tholeiites to olivine melilites from SE Australia utilizing geochemical and experimental petrological data. Jour. Petrol., v. 19, pp. 463-513.

Gautam, G.C. and Srivastava, R.K. (2011). Petrology, geochemistry and petrogenesis of early Precambrian mafic dyke swarm from Dondi-Bhanupratappur-Keshkal, central Bastar craton, India. *In*: Srivastava, R.K. (Ed.), Dyke swarms: keys for geodynamic interpretation. Springer-Verlag, Heidelberg, pp. 203-218. doi:10.1007/978-3-642-12496-9_12

Geldmacher, J., Haase, K.M., Devey, C.W. and Garbe-Schönberg, C.D. (1998). The petrogenesis of Tertiary cone-sheets in Ardnamurchan, NW Scotland: petrological and geochemical constraints on crustal contamination and partial melting. Contrib. Mineral. Petrol., v. 131, pp. 196-209. doi:10.1007/S004100050388

Green, D.H. (1971). Composition of basaltic magmas as indicators of conditions of origin application to oceanic volcanism. Philos. Trans. Roy. Soc. London, v. 268, pp. 707-725.

GSI (2001). District resource map of Gadchiroli district, Maharashtra. Geol. Surv. India, Central Region, Nagpur.

Haase, K.M. (1996). The relationship between the age of the lithosphere and the composition of oceanic magmas constraints on partial melting, mantle sources and the thermal structure of the plates. Earth Planet. Sci. Lett., v. 144, pp. 75-92.

Haggerty, S.E. (1995). Upper mantle mineralogy. Jour. Geodynamics, v. 20, pp. 331-364.

Hall, R.P. and Hughes, D.J. (1987). Norite dykes of southern Greenland: early Proterozoic boninitic magmatism. Contrib. Mineral. Petrol., v. 97, pp. 169-182. doi: 10.1007/BF00371237

Halls, H.C. (1987). Dyke swarms and continental rifting: some concluding

remarks. *In*: Halls, H.C. and Fahrig, W.F. (*Eds.*), Mafic dyke swarms. Geol. Asso. Canada Spec. Pap, v. 34, pp. 483-492.

Hatton, C.J. and Sharpe, M.R. (1989). Significance and origin of boninite-like rocks associated with the Bushveld complex. *In*: Crawford, A.J. (*Ed.*), Boninites and Related Rocks. Unwin Hyman, London, pp. 174-207.

Hawkesworth, C.J. and Gallagher, K. (1993). Mantle hotspot plume and regional tectonics as cause of interpolate magmatism. Terra Nova, v. 5, pp. 552-559. doi:10.1111/J.1365-3121.

Hazarika, B., Malpe, D.B. and Dongre, A.N. (2019). Petrology and geochemistry of a boninite dyke from the western Bastar craton of Central India. Jour. Earth Syst. Sci., v. 128, pp. 1-17. doi:10.1007/s12040-018-1052-y

Hazarika, B., Malpe, D.B. and Dongre, A.N. (2020). Petrogenesis of mafic dykes from the western Bastar craton of Central India and their relation to outgrowth of Columbia supercontinent. Mineral. Petrol., v. 114, pp. 243-262. doi: 10.1007/s00710-020-00695-y

Herzberg, C. (1992). Depth and degree of melting of Komatite. Jour. Geophy. Res., v. 97, pp. 4521-4540.

Herzberg, C. (1995). Generation of plume magma through time: an experimental perspective. Chem. Geol., v. 126, pp. 1-16.

Horan, M.F., Hanson G.N. and Spencer, K.J. (1987). Pb and Nb isotope and trace constraints on the origin of basic rocks in an early Proterozoic igneous complex. Minnesota. Precamb. Res., v. 37, pp. 323-342.

Hsean, A.R., Karkare, S.G., Singh, R.K., Chandra, R. and Srivastava , R.K. (2003). Petrochemistry of precambrian granitoids of the Katekalyan, Southern Bastar Carton, Central India. *In:* Kuity, D.P. and Divakar Rao, V. (*Eds.*), Granites and Associated Mineralization. Hindustan Publication, New Delhi, pp.217-234.

Irvine, T.N. and Baragar, W.R.A. (1971). A guide to the chemical classification of the common volcanic rocks. Can. Jour. Earth Sci., v. 8, pp. 523-548.

Jensen, L.S. (1976). A new cation plot for classifying sub-alkaline volcanic rocks. Ontario Division Mines Ministry of Natural Resources Misc Paper, 22p.

Kent, R.W. and Fitton, J.G. (2000). Mantle source and melting dynamics in the British Palaeogene igneous province. Jour. Petrol., v. 41, pp. 1023-1040.

Lassiter, J.C. and DePaolo, D.J. (1997). Plume/lithosphere interaction in the generation of continental and oceanic flood basalt: chemical and isotopic constraints. *In*: Large igneous provinces: Continental and oceanic and planetary flood volcanism. Geophy. Monograph, v. 100, pp. 335-355.

Le Bas, M.J., Le Maitre, R.W., Streckeisen, A. and Zanettin, B. (1986). A chemical classification of volcanic rocks based on the total alkali-silica diagram. Jour. Petrol., v. 27, pp. 745-750.

LeCheminant, N.A. and Heaman, L.M. (1989). Mackenzie igneous events, Canada: middle Proterozoic hotspot magmatism associated with ocean opening. Earth Planet. Sci. Lett., v. 96, pp. 38-48.

Liao, A.C., Shellnutt, J.G., Hari, K.R., Denyszyn, S.W., Vishwakarma, N. and Verma, C.B. (2019). A petrogenetic relationship between 2.37 Ga boninitic dyke swarms of the Indian shield: evidence from the central Bastar craton and the NE Dharwar craton. Gond. Res., v. 69, pp. 193-211.

McDermott, F., Defant, M.J., Hawkesworth, C.J., Maury, R.C. and Joron, J.L. (1993). Isotope and trace element evidence for three component mixing in the genesis of the North Luzon arc lavas (Philippines). Contrib. Miner. Petrol., v. 113, pp. 9-23.

McDonough, W.F., Sun, S.S., Ringwood, A.E., Jagoutz, E. and Hofmann, A.W. (1992). K, Rb and Cs in the earth and moon and the evolution of the earth's mantle. Geochim. et. Cosmochim. Acta, v. 56, pp. 1001-1012.

Mohr, P.A. (1987). Crustal contamination in mafic sheets: a summary. In: Halls, H.C. and Fahriig, W.F. (Eds.), Mafic Dyke Swarms, Geol. Asso. Canada Spec. Paper v. 34, pp. 75-80.

Murthy, N.G.K. (1987). Mafic dyke swarms of the Indian shield. *In*: Halls, H.C. and Fahriig, W.F. (Eds.), Mafic Dyke Swarms, Geol. Asso. Canada Spec. Paper v. 34, pp. 393-400.

Neogi, S., Miura, H. and Hariya, Y. (1996). Geochemistry of the Dongargarh volcanic rocks, Central India: implications for the Precambrian mantle. Precamb. Res., v. 76, pp. 77-91.

Paz Moreno, F.A. and Demant, A. (1999). The Recent Isla San Luis volcanic centre: petrology of a rift-related volcanic suite in the northern Gulf of California. Jour. Volcano. Geotherm. Res., v. 93, pp. 31-52.

Pearce, J.A. (2008). Geochemical fingerprinting of oceanic basalts with applications to ophiolite classification and the search for Archaean oceanic crust. Lithos, v. 100, pp. 14-48.

Pearce, J.A. (1982) Trace element characteristics of lavas from destructive plate boundaries. *In*: Thorpe, R.S. (*Ed.*), Andesites, Wiley, Hoboken, pp. 528-548.

Pearce, J.A. and Norry, M.J. (1979). Petrogenetic implications of Ti, Zr, Y and Nb variation in volcanic rocks. Contrib. Mineral. Petrol., v. 69, pp. 33-47.

Piercey, S.J., Murphy, D.C., Mortensen, J.K. and Paradis, S. (2001). Boninite magmatism in a continental margin setting, Yukon-Tanana terrane, southeastern Yukon, Canada. Geol., v. 29, pp. 731-734.

Pisarevsky, S.A., Biswal, T.K., Wang, X.C., DeWaele, B., Ernst, R., Söderlund, U., Tait, J.A., Ratre, K., Singh, Y.K. and Cleve, M. (2013). Palaeomagnetic, geochronological and geochemical study of Mesoproterozoic Lakhna dykes in the Bastar craton, India: implications for the Mesoproterozoic supercontinent. Lithos, v. 174, pp. 125-143.

Poidevin, J.L. (1994). Boninite-like rocks from the Palaeoproterozoic greenstone belt of Bogoin, Central African Republic: geochemistry and petrogenesis. Precamb. Res., v. 68, pp. 97-113.

Puchtel, I.S., Arndt, N.T., Hofmann, A.W., Haase, K.M., Kröner, A., Kulikov, V.S., Kulikova, V.V., Garbe-Schönberg, C.D. and Nemchin, A.A. (1998). Petrology of mafic lavas within the Onega plateau, Central Karelia: evidence for 2.0 Ga plume related continental crustal growth in the Baltic shield. Contrib. Mineral. Petrol., v. 130, pp. 134-153.

Puchtel, I.S., Haase, K.M., Hofmann, A.W., Chauvel, C., Kulikov, V.S., Garbe-Schonberg C.D. and Nemchin, A.A. (1997). Petrology and geochemistry of crustally contaminated komatitic basalt from the Vetreny Belt, southeastern Baltic shield: Evidence for an early Proterozoic mantle plume beneath rifted Archean continental lithosphere. Geochim. et. Cosmochim. Acta, v. 61, pp. 1205-1222.

Ramachandra, H.M., Mishra, V.P. and Deshmukh, S.S. (1995). Mafic dykes in Bastar Precambrian: study of the Bhanupratappur-Keshkal mafic dyke swarms. Geol. Soc. India Memoir v. 33, pp. 183-208.

Ratre, K., De Waele, B., Biswal, T.K. and Sinha, S. (2010). SHRIMP geochronology for the 1450 ma Lakhna dyke swarm: its implication for the presence of Eoarchean crust in the Bastar craton and 1450-517 ma depositional age for Purana basin (Khariar), eastern Indian peninsula. Jour. Asian Earth Sci., v. 39, pp. 565-577.

Rogers, J.W. and Santosh, M. (2002). Configuration of Columbia, a Mesoproterozoic supercontinent. Gond. Res., v. 5, pp. 5-22.

Samal, A.K., Srivastava, R.K., Ernst, R.E. and Söderlund, U. (2019). Neoarchean-Mesoproterozoic mafic dyke swarms of the Indian shield mapped using Google earth™ images and ArcGIS™, and links with large igneous provinces. *In*: Srivastava, R.K., Ernst, R. and Peng, P. (*Eds.*), Dyke swarms of the world: a modern perspective, Springer Nature Singapore Pvt Ltd., pp. 335-390.

Sarkar, A., Sarkar, G., Paul, D.K. and Mitra, N.D. (1990). Precambrian geochronology of Central Indian Shield-A review. Geol. Surv. India, v. 122, pp. 29-30.

Shashidharan, K., Mohanty, A.K. and Gupta, A. (2002). A note on incidence of diamond in Wairagarh metasedimentary rocks, Garhchiroli district, Maharashtra. Jour. Geol. Soc. India, v. 59, pp. 265-270.

Shellnutt, J.G., Hari, K.R., Liao, A.C., Denyszyn, S.W. and Vishwakarma, N. (2018). A 1.88 Ga giant radiating mafic dyke swarm across southern India and western Australia. Precamb. Res., v. 308, pp. 58-74.

Smithies, R.H. (2002). Archaean boninite-like rocks in an intracratonic setting. Earth Planet. Sci. Lett., v. 197, pp. 19-34.

Srivastava, R.K. (2006). Geochemistry and petrogenesis of Neoarchaean high-Mg low-Ti mafic igneous rocks in an intracratonic setting, Central India craton: evidence for boninite magmatism. Geochem. Jour., v. 40, pp. 15-31.

Srivastava, R.K. (2008). Global intracratonic boninite-norite magmatism during the Neoarchean-Palaeoproterozoic: evidence from the central Indian Bastar craton. Inter. Geol. Rev., v. 50, pp. 61-74.

Srivastava, R.K. (2011). Dyke swarms: keys for geodynamic interpretation. Springer- Verlag, Heidelburg, 637p.

Srivastava, R.K. and Gautam, G.C. (2008). Precambrian mafic dyke swarms from the southern Bastar craton, central India: present and future perspectives. *In*: Srivastava, R.K., Sivaji, C. and Chalapathi Rao, N.V. (Eds.), Indian Dyke: Geochemistry, Geophysics and Geochronology, Narosa Publishing House Pvt Ltd.: New Delhi; pp. 367-376.

Srivastava, R.K. and Gautam, G.C. (2012). Early Precambrian mafic dyke swarms from the central Archaean Bastar craton, India: geochemistry, petrogenesis and tectonic implications. Geol Jour., v. 47, pp. 144-160.

Srivastava, R.K. and Gautam, G.C. (2015). Geochemistry and petrogenesis of Paleo-Mesoproterozoic mafic dyke swarms from northern Bastar craton, Central India: geodynamic implication in reference to Columbia supercontinent. Gond. Res., v. 28, pp. 1061-1078.

Srivastava, R.K. and Singh, R.K. (2004). Trace element geochemistry and genesis of Precambrian sub-alkaline mafic dikes from the central Indian craton: evidence for mantle metasomatism. Jour. Asian Earth Sci., v. 23, pp. 373-389.

Srivastava, R.K., Hall, R.P., Verma, R. and Singh, R.K. (1996). Contrasting Precambrian mafic dykes of the Bastar craton, Central India: petrological and geochemical characteristics. Jour. Geol. Soc. India, v. 48, pp. 537-546.

Srivastava, R.K., Heaman, L.M., French, J.E. and Filho, C.F.F. (2011). Evidence for a Paleoproterozic event of metamorphism in the Bastar craton, Central India: P-T-t constraints from mineral chemistry and U-Pb geochronology of mafic dykes. Episodes, v. 34, pp. 13-24.

Srivastava, R.K., Pimentel, M.M. and Gautam, G.C. (2016). Nd isotope and geochemistry of an early Palaeoproterozoic high-Si high-Mg boninite-norite suite of rocks in the southern Bastar craton, Central India: petrogenesis and tectonic significance. Inter. Geol. Rev., v. 58, pp. 1596-1615.

Srivastava, R.K., Söderlund, U., Ernst, R.E., Mondal, S.K. and Samal, A.K. (2019). Precambrian mafic dyke swarms in the Singhbhum craton (eastern India) and their links with dyke swarms of the eastern Dharwar craton (southern India). Precamb. Res., v. 329, pp. 5-17.

Srivastava, R.K. and Samal, A.K. (2019). Geochemical characterization, petrogenesis, and emplacement tectonics of Paleoproterozoic high-Ti and low-Ti mafic intrusive rocks from the western Arunachal Himalaya, northeastern India and their possible relation to the ~1.9 Ga LIP event of the Indian shield. Geol. Jour., v. 54, pp. 245-265.

Subba Rao, D.V., Khan, M.W.Y., Sridhar, D.N. and Nagaraju, K. (2007). A new find of dolerite dykes with continental flood basalt affinity from the Meso-Neoarchaean Chhattisgarh basin, Bastar craton, Central India. Jour. Geol. Soc. India, v. 69, pp. 80-84.

Subba Rao, D.V., Sridhar, D.N., Balaram, V., Nagaraju, K., Rao, T.G., Keshavakrishna, A. and Singh, U.P. (2008). Proterozoic mafic-ultramafic dyke swarms in the vicinity of Chhattisgarh-Khariar-Singhora basins in northern Bastar craton, Central India. *In*: Srivastava, R.K., Sivaji, C. and Chalapathi Rao, N.V. (Eds.), Indian dykes: geochemistry, geophysics and geochronology. Narosa Publishing House Pvt. Ltd., New Delhi, pp. 377-396.

Tarney, J. and Weaver, B.L. (1987). Geochemistry and petrogenesis of early Proterozoic dyke swarms, *In*: Halls, H.C. and Fahriig, W.F. (Eds.), Mafic Dyke Swarms, Geol. Asso. Canada Spec. Paper, v. 34, pp. 81-94.

Vijaya Kumar, K., Laxman, M.B. and Nagaraju, K. (2018). Mantle source heterogeneity in continental mafic Large Igneous Provinces: insights from the Panjal, Rajmahal and Deccan basalts, India. Geol. Soc. London, Spec. Publ., v. 463(1), pp. 87-116. doi:10.1144/SP463.5

Weaver, B.L. and Tarney, J. (1984). Estimating the composition of the continental crust: an empirical approach. Nature, v. 310, pp. 575-577.

Yellappa, T., Chetty, T.R.K. and Santosh, M. (2012). Tectonic framework of southern Bastar craton, Central India: a study based on different spatial information data sets. Geol. Jour., v. 47(2,3), pp. 161-185.

Zhao, J.H. and Zhou, M.F. (2007). Geochemistry of Neoproterozoic mafic intrusions in the Panzhihua district (Sichuan Province, SW China): implications for subduction-related metasomatism in the upper mantle. Precamb. Res., v. 152, pp. 27-47.